sciendo
ISSN 1335-8871
MEASUREMENT SCIENCE REVIEW
Journal homepage: https://content.sciendo.com

Design of Calibration System for Multi-Channel Thermostatic Metal Bath

Hua Zhuo[1,2*], Yan Xu[3], Weihu Zhou[4], Feng Li[2], Yikun Zhao[2]

[1]*Instrument Science and Technology, Department of Automation, Nanjing University of Aeronautics and Astronautics, No. 29, Jiangjun Avenue, Jiangning District, Nanjing City, 211106, Jiangsu Province, China, zhuoxiaobingling@sina.com*
[2]*Thermal Metrology Testing Institute, Xinjiang Uygur Autonomous Region Research Institute of Measurement & Testing, Hebei Street, No.258, 830011, Urumqi, China, li_1221@sina.com, ykzhao2005@sina.com*
[3]*School of Mechanical Engineering, Xinjiang University, Xinjiang University Boduo Campus, No. 777, Huarui Street, Shuimogou District, Urumqi, Xinjiang., 830011, Urumqi, China, lilixiu_z@163.com*
[4]*Institute of Microelectronics, Chinese Academy of Sciences, University of Chinese Academy of Sciences, 9 Dengzhuang South Road, Haidian District, Beijing, 100094, China, zhouweihu@ime.ac.cn*

Abstract: The use of the thermostatic metal bath is becoming more and more extensive and the requirements for its precision and reliability are also increasing. To meet the needs of the metal bath calibration, a 12-channel thermostatic metal bath temperature field calibration system based on a four-wire PT100 has been designed. The system design includes a front-end temperature measurement component, which consists of a four-wire PT100 and a thermostatic block, and a signal processing component, which consists of a bidirectional constant current source excitation unit, a signal conditioning unit and a high-precision acquisition unit. The STM32f407 is used as the main control chip, and the analog channel selector is used for 12-channel selection. The constant current source is used for signal excitation, the proportional method is used to measure the PT100 resistance, and an acquisition circuit with a high-precision 32-bit ADS1263 analog-to-digital converter is used to amplify, filter and convert the analog signal. After piecewise linear fitting and system calibration, the temperature measurement accuracy can reach 0.4 mK, which meets the calibration requirements of the thermostatic metal bath.

Keywords: thermostatic metal bath, high-precision temperature measurement, PT100, multi-channel temperature measurement.

1. INTRODUCTION

The thermostatic metal bath is a product that uses the numerical control heating method and semiconductor cooling technology to provide stable control of the metallic module temperature. This product replaces the traditional constant temperature water (oil) bath device and has the advantages of rapid heating, high temperature control precision and good uniformity. At the same time, different metallic modules can be used to adapt to different tests, so it is widely used in enzyme preparation reaction tests, serum inactivation tests, Rh blood sample research, cross-matching blood, enzyme digestion, protein denaturation, PCR pre-reaction, cholesterol denaturation identification and testing and other fields in the entire pharmaceutical, chemical, food safety, quality control, environmental and other industries.

The temperature control range, heating time, temperature stability, module temperature uniformity and other technical indicators of the thermostatic metal bath directly affect the quality of the preserved samples and the test accuracy. Therefore, the temperature deviation, fluctuation and uniformity of the dry-body thermostat are considered important measurement parameters. The current metal bath calibration methods and systems [1]-[3] generally use a single-hole measurement, and the probe must be set up in advance. It may fail to record or record unsuccessfully during use, and reading the data after calibration reduces the reliability. The upper cover must be opened when measuring, so the measurement will result in air flow in the hole and the surrounding air, which not only does not match the hole diameter of the metal bath module, but is also easily affected by the ambient temperature. Due to the inability to compensate, there will be a large error in temperature detection, and it is impossible to detect the entire temperature field, spatial difference, heating rate, etc. In the state of the art, there is also a wireless metal bath temperature field calibration set-up that uses a single-channel measurement. If multiple hole positions are to be measured simultaneously, multiple devices must be placed. Since it is impossible to control multiple devices at the same time, and the measurement time of multiple devices cannot be kept consistent, the measurement accuracy and reliability are reduced.

DOI: 10.2478/msr-2024-0004
*Corresponding author: zhuoxiaobingling@sina.com (H. Zhuo)

For a high-precision temperature measurement device, a constant voltage bridge circuit composed of a negative temperature coefficient thermistor and a resistive divider is used to acquire 8 channels of temperature data [4], and a constant current source was developed to stimulate the PT100 using the dual-ADC temperature measurement method to perform signal acquisition [5]. In comparison with the thermocouple and thermistor temperature sensor, the high-precision temperature measurement system of PT100 is widely used in different types because of its wide temperature measurement range, good linearity and high stability. The semiconductor cooler controls the temperature of the bidirectional constant current source to improve the precision of temperature measurement [6]. To overcome the shortcomings of speed or accuracy degradation in the multi-channel scanning mode, a resistance-proportional temperature acquisition device with a cyclic structure based on a high-precision ADC is used [7]. In addition, there is an active bridge system to ensure the Pt resistor temperature measurement range [8]. Since the temperature measurement of the Pt resistor has a non-linear error, a mixed-mode linearization method with a special two-stage piecewise linear ADC was designed to reduce the non-linear error of the Pt resistor [9]. In a high-precision voltage measurement system, the offset and temperature offset of the device are usually the most important factors affecting the temperature measurement precision. Therefore, a bidirectional constant current source is used in this system, that is, it controls the generation of a constant current source with equal and opposite directions to ground to stimulate each resistor and generate a voltage signal that reduces the error caused by the offset voltage. At the same time, the resistance ratio method is used, that is, the reference resistor with high precision and low temperature drift is connected in series with the Pt resistor to eliminate the constant current source coefficient and reduce the influence of the temperature drift of the constant current source on the system, and the linear regression method is used for temperature calibration and compensation [10]-[12]. Finally, the requirements of miniaturization, convenience, high precision and high efficiency calibration are met in practical applications.

2. FINITE ELEMENT ANALYSIS OF TEMPERATURE FIELD IN A THERMOSTATIC METAL BATH

To obtain a reasonable solution for the verification of the thermostatic metal bath, the thermostatic metal bath temperature distribution characteristics are first determined by finite element analysis to study the influence of the environment on the metal bath temperature field and determine the overall distribution of the measuring points. The temperature field simulation process includes the creation of the geometric model, the meshing, the definition of the boundary conditions, the calculation results and the post-processing analysis. In this paper, a specific type of thermostatic metal bath is taken as an example. The three-dimensional geometric model is shown in Fig. 1. The model includes the shell, the calculation module and the heating film. The metallic module is made of a high-density aluminum alloy and the shell is made of phenolic plastic to ensure the temperature uniformity of the thermal block. The thermal properties of each area are listed in Table 1. Then the structure, heating mode and heat transfer mode are analyzed. The heating condition is the heating of the heating film at the bottom of the metallic module and the temperature change is taken as the boundary condition, which is measured by the internal sensor of the thermostatic metal bath [13], [14].

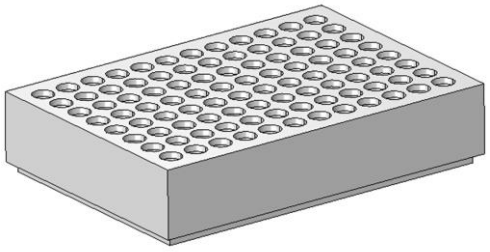

Fig. 1. 3D structure of the thermostatic metal bath.

Table 1. Material parameters for each region in the module.

Component	Material name	Density (kg/m^3)	Specific heat capacity $J/(kg \cdot K)$	Thermal conductivity $W/(m \cdot K)$
metallic module	aluminum	2719	871	202.4
base	bakelite	1260	1464	0.186

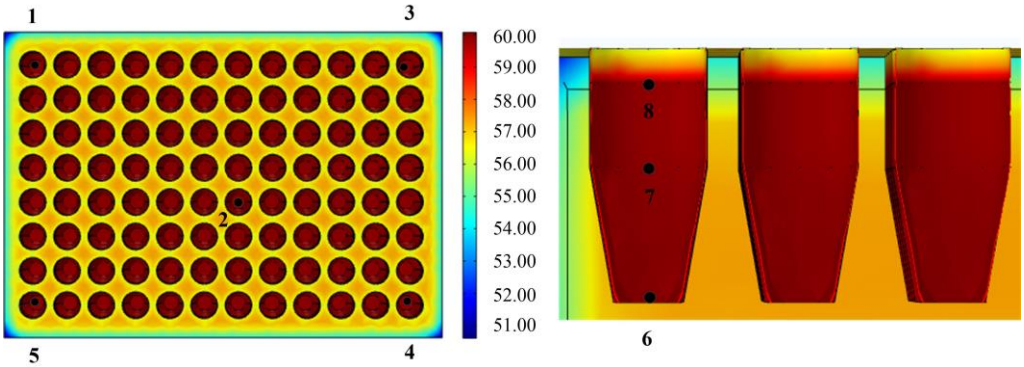

Fig. 2. Cloud of the 60 °C temperature field in a thermostatic metal bath.

The cloud of the 60 ℃ temperature field in a thermostatic metal bath is shown in Fig. 2. The temperature measurement is performed at the bottom of five wells of the metal bath and three parts of the well, as shown in Fig. 2. The temperature difference of the bottom of well 2 and wells 1, 3, 4, 5 is 0.06-0.07 ℃, indicating that the temperature in the hole of the metal bath is uneven. The temperature difference between the bottom of hole 1 and the top is 0.06 ℃. From this result, it can be concluded that the thermostatic metal bath is greatly affected by the air, and the temperature of the bottom, center, and top of the hole has a downward trend. Therefore, when designing the calibration set-up of the metal bath, it is necessary to ensure that the temperature probe touches the bottom of the metal hole during measurement, and the measurement hole must be sealed to reduce the influence of the environment so that the temperature of the metal bath can be measured.

3. HARDWARE DESIGN

Based on the 12-channel thermostatic metal bath temperature field calibration system with four-wire PT100, the method for measuring voltage with a constant current source is used in the calibration set-up. It consists of a sensor module, a signal excitation module, a signal collection module, a control and processing module, a power supply module and an interaction module, and requires that the temperature can be acquired and stored with high precision. The temperature measurement range is -50~150 ℃, and the measurement error is less than 1 mK. A class A PT100 resistor is used as the sensitive element and the resistance within the measured temperature range is 70~160 Ω. The self-heating coefficient is 0.01524℃/mW, and the temperature coefficient of the resistor is 0.003851 Ω/℃. Further parameters of the Pt100 are listed in Table 2. Fig. 3 shows the overall structure of the proposed system.

Table 2. PT100 parameter table.

Probe material	Probe accuracy	Probe length (mm)	Probe diameter (mm)	Self-heating coefficient (℃/ mW)	Temperature coefficient of the resistor (Ω/℃)
304 stainless steel	Grade A	30	5	0.01524	0.003851

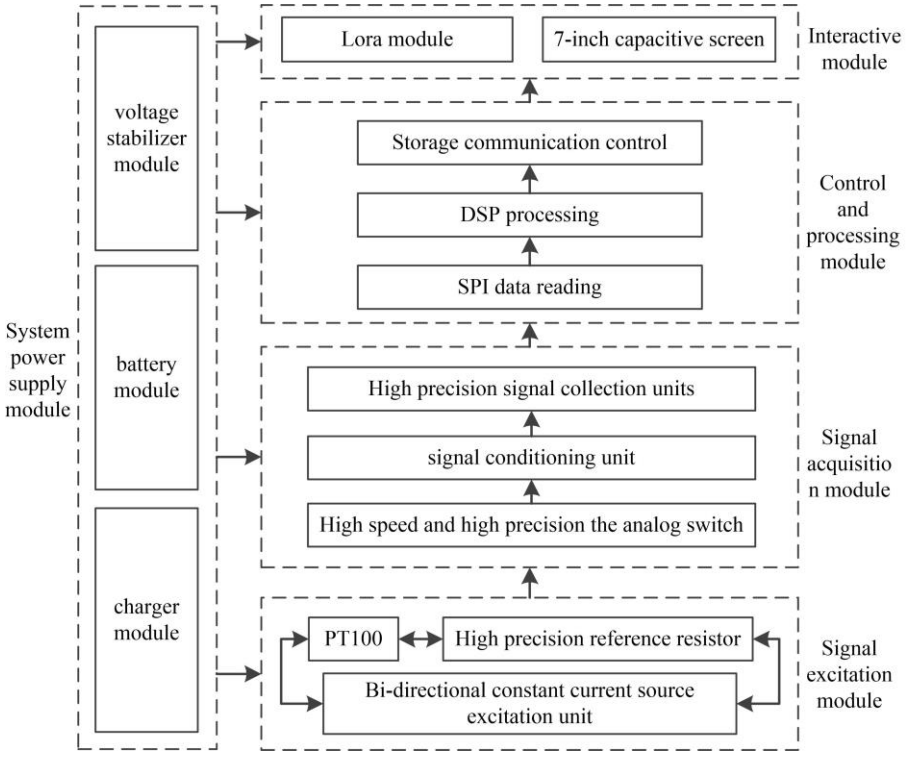

Fig. 3. Overall structure of the proposed system.

1) Signal excitation module:

In this module, the sensor uses a class A PT100 four-wire platinum resistor. The platinum resistor is characterized by high precision and rapid response. Simultaneously, the four-wire configuration completely eliminates the influence of lead resistance, which increases the accuracy of temperature acquisition. A constant current source provides a constant current excitation to both the PT100 platinum resistor and the reference resistor and converts temperature into a voltage signal. A bi-directional constant current source is used to eliminate the circuit offset voltage: the forward current flows from the PT100 platinum resistor through the reference resistor, while the reverse current flows from the reference resistor to the PT100 platinum resistor.

2) Signal excitation module:

The constant current source provides a constant current excitation for the PT100 resistor and reference resistor and converts the temperature into a voltage signal. The bidirectional constant current source is used to compensate for the offset voltage of the circuit. The forward current flows from the PT100 resistor through the reference resistor, while the reverse current flows from the reference resistor to the PT100 resistor.

The resistance of the PT100 resistor can be calculated by:

$$R_t = \frac{U_{Rt+} - U_{Rt-}}{U_{\text{Rref+}} - U_{\text{Rref-}}} \times R_{\text{ref}} \quad (1)$$

where R_t is the resistance of the thermistor; R_{ref} is the resistance of the reference resistor; UR_{t+} and U_{Rt}-are voltages across the PT100 resistor with positive and negative current excitation, respectively; U_{Rref+} and U_{Rref-} are voltages across the reference resistor with positive and negative current excitation, respectively.

3) Signal collection module:

The single-chip microcomputer selects the acquisition channel by controlling the analog switch and reads the voltage signal of the selected channel, which is collected by the ADC after filtering, noise reduction and amplification. This system ADC chip uses the high-precision 32-bit ADS1263 with programmable gain amplifier (PGA), voltage reference and internal error monitoring. Two identical synchronous acquisition circuits are used to acquire the voltage signals at both ends of the PT100 resistor and the reference resistor, which can effectively eliminate the error caused by the fluctuation of the excitation current of the constant current source. By changing the current direction, each resistor is detected multiple times, and then the median filtering method is used to reduce the error caused by the stray potential.

4) Control and processing module:

The STM32f407 is used as the main control chip in this design, with a built-in CortexTM-M4 high-performance core with a frequency of 168 MHz, which reads the data collected by the ADC via the SPI interface. The data is converted into temperature after compensation processing by the internal DSP, thus fulfilling the core computation requirements of the proposed temperature measurement system.

5) Interaction module:

A 7-inch capacitive screen is used for human-computer interaction, while LORA and the host computer are used for wireless communication.

6) Power supply module:

Li-on batteries are used to power the system, using a Coulomb meter for power measurement, and to separate analog and digital power supplies. The different analog and digital power supplies are separated at the power layer to improve the power quality.

Fig. 4 shows the designed PCB board.

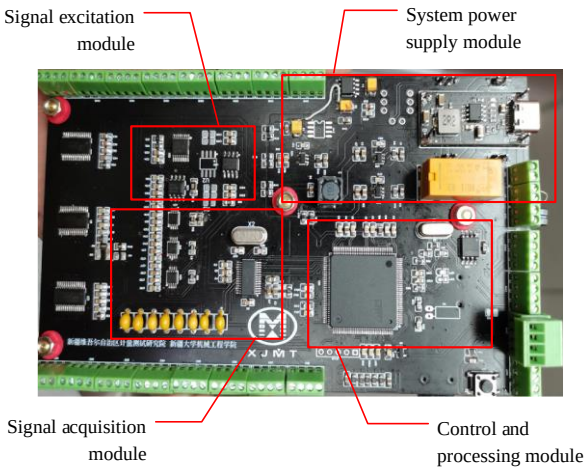

Fig. 4. Image of the designed PCB.

A. Design of temperature measurement component

The temperature measurement component includes a PT100 resistor and multiple thermostatic blocks. This design uses the class A four-wire PT100 resistor, which is characterized by high precision and rapid response. Meanwhile, the four-wire can completely eliminate the influence of lead resistance and improve temperature measurement. A constant current is applied to the "q" and "w" terminals for excitation, and the voltage is measured at "+" and "-" terminals, as shown in Fig. 5.

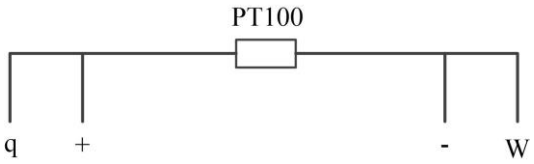

Fig. 5. Schematic of PT100 wiring.

A major difficulty in calibrating thermostatic metal baths is that there are many types of metal bath mold structures, and the size, aperture and bottom shape of metal bath modules are quite different. The traditional calibration methods include:

1. A single temperature sensor used to check and measure the bottom of the metal module hole when the cover is open.
2. Thermal oil or thermal grease added to the metal bath hole to match the temperature sensor to open the cover for calibration.
3. A matching test tube inserted into the hole of the metal bath, and thermal oil or thermal grease added to the test tube to match the temperature sensor for calibration.

The current measurement methods can only detect one or a specific type of metal bath module, have limited adaptability and are easily affected by the ambient temperature, resulting in large errors in temperature detection, and cannot measure the entire temperature field and spatial differences, heating rate, etc. In this design, a conical thermostatic block made of silicone is used, which can be adapted to a variety of metal bath modules with different apertures, keeping the hole as tightly sealed as

possible, avoiding heat loss and ambient temperature during the measurement process. A schematic diagram of the thermostatic block structure is shown in Fig. 6.

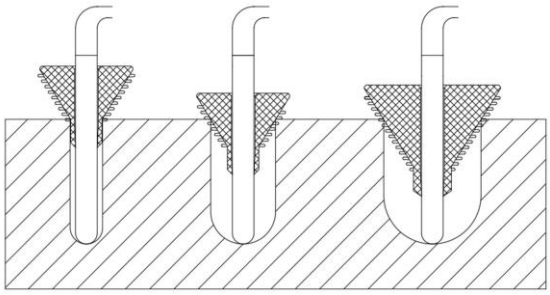

Fig. 6. Schematic of a thermostatic block.

The conical silicone thermostatic block can adapt to different aperture sizes and ensure accurate temperature measurement by bringing the thermally conductive oil into full contact with the bottom of the hole. Without the use of the thermostatic block, the temperature difference at 200 °C can reach about 3 °C.

B. Design of bidirectional constant current source excitation unit

The constant current source provides a bidirectional constant current excitation for the PT100 resistor and the reference resistor. Considering the self-heating effect of the PT100 resistor, the excitation current must not exceed 1 mA and the design value is 0.3 mA. Fig. 7 illustrates the working principle of the constant current source excitation circuit.

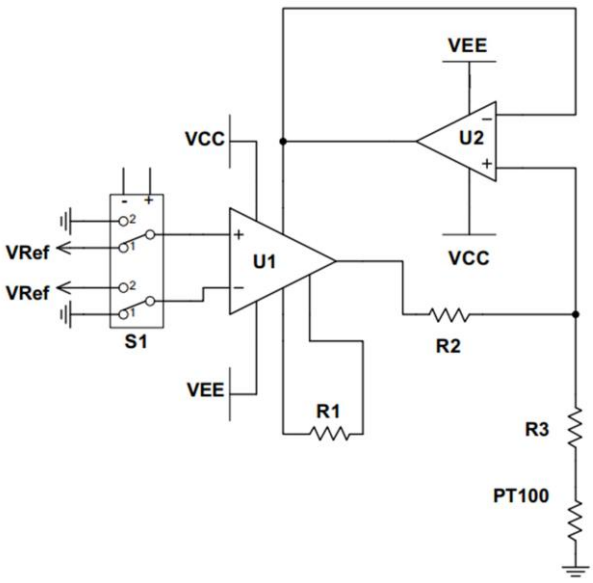

Fig. 7. Working principle of the constant current source excitation circuit.

S1 is the output current direction switch. The MCU controls the precision reference voltage source of 2.5 V by controlling the switch S1 and passes it to U1 in different input directions. The high-precision instrumentation operational amplifier U1 and the precision operational amplifier amp U2 are combined in a negative feedback mode, where U2 is the output follower operational amplifier and the output voltage of U1 is fed back to the reference terminal of U2 after passing through resistor R2.

An INA333 high-precision instrument is used as the operational amplifier in U1, and the input magnification G can be calculated using (2):

$$G = 1 + \frac{100_{\mathrm{K\Omega}}}{R_1} \tag{2}$$

where R_1 is the operational amplifier gain of the resistor.

If S1 is disconnected, i.e., the forward input terminal of U1 is connected to the 2.5 V reverse input terminal and earthed. If the circuit is stable, the output current can be calculated by:

$$I_{out} = \frac{G(V_{1+} - V_{1-})}{R_2} \tag{3}$$

where V_{1+} and V_{1+} are the forward and reverse inputs of U_1, respectively; R_2 is the current-regulating resistor.

When S1 is switched off, the current flows from the PT100 resistor to the reference resistor. When S1 is switched on, the current flows from the reference resistor to the PT100 resistor, creating a bidirectional constant current source. Since this system is a ratio measurement method, the requirements for the precision, temperature drift and input bias current of the constant current source are not high. Therefore, the noise performance of the device is the primary consideration when selecting the device. In this system, the low-noise, low temperature drift high-precision voltage reference chip ADR421 is selected to generate a voltage of 2.5 V as the Vref input, and the total noise is only 1.75 mV. The high-precision instrument INA333 is used as the operational amplifier in U_1. The OPA333 precision and zero drift amplifier is used for U_2. A high-precision resistor is used as the resistor, where R_1 = 25 kΩ, R_2 = 10 kΩ and the output current I_{out} is 0.3 mA.

C. Design of the signal conditioning unit

Low-noise signals are the key to ensuring the temperature measurement accuracy of the system. The signal conditioning unit performs filtering and noise reduction processing of the front-end voltage signal. To accurately capture the bidirectional voltage through the ADC, a conditioning circuit with a common-mode voltage of 2.5 V was developed. Fig. 8 shows the circuit.

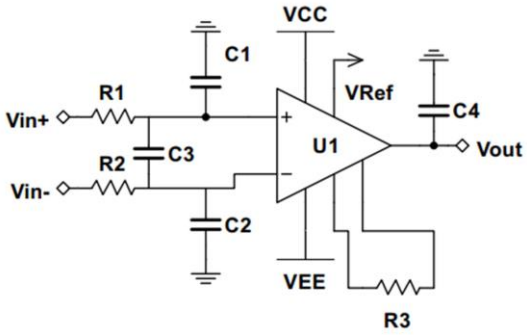

Fig. 8. Principles of the signal conditioning circuit.

U1 is the instrumentation amplifier, characterized by a high input impedance and a high common-mode rejection ratio, which can be calculated by (2). When the gain is G, its output voltage can be calculated by:

$$V_{out} = G(V_{in+} - V_{in-}) + V_{\text{ref}} \tag{4}$$

where V_{in+} and V_{in-} are the voltages at the input of the PT100 resistor and the reference resistor, respectively; V_{ref} is the reference voltage (2.5 V in this case).

C_1, C_2, and C_3 are filter capacitors, which can ensure a relatively gentle capturing of the bidirectional voltage, and the cut-off frequency can be calculated by:

$$f = \frac{1}{2\pi RC} \tag{5}$$

where R is the filter resistance and refers to R1 and R2 in this article; C is the filter capacitance and refers to C1 and C2 in this article.

With a design cut-off frequency of 20 Hz, the passband increase A can be calculated by:

$$A = 1 + \frac{100K\Omega}{R_3} \tag{6}$$

where R_3 is the operational amplifier gain of the resistor.

To ensure the system stability and suppress high-frequency noise, the design cut-off frequency is 20 Hz, i.e., $R_1 = R_2 = 80$ KΩ, $C_1 = C_2 = C_3 = 0.1$ μF. At the same time, the resistance of the reference resistor is set to 100 Ω, i.e., the conditioning circuit of the PT100 and the reference resistor can be exactly the same. The resistance within the temperature range measured by the PT100 resistor is 70~160 Ω. According to Ohm's law, the required measurement range is 35~80 mV, and $A = 25$, $R_3 = 4$ kΩ.

D. Design of a high-precision signal collection unit

According to the requirements of temperature measurement accuracy and the range of the PT100 resistor resistance, it can be calculated that the equivalent voltage resolution is 4.8 μV with a current excitation of 0.3 mA from (7). It can then be calculated from (8) that the noise-free bits of the required ADC device are at least 19 bits.

$$\Delta V = \alpha \cdot K \cdot \mathrm{I} \cdot A \tag{7}$$

$$B = \log_2^{\frac{V_{\text{ref}}}{\Delta V}} \tag{8}$$

where α is the sensitivity coefficient of the PT100 resistor (0.3851 Ω/°C in this case). K is the required temperature measurement resolution (0.001 °C in this case). I is the constant current source (0.3 mA in this case). A is amplification (25 in this case). B is the noise-free bit of the ADC device (unit = bit). V_{ref} is the reference voltage (2.5 V in this case). ΔV is the equivalent voltage resolution.

In this system, a 32-bit ΔΣ ADC is selected as a high-precision signal acquisition device, and its model is ADS1263. The ADC consists of a low-noise CMOS PGA, a ΔΣ modulator and a programmable digital filter. The front-end CMOS PGA consists of two chopper-stabilized amplifiers and a resistor network to configure the gain, and the input is equipped with a high-frequency electromagnetic interference (EMI) filter.

The ADC's internal programmable digital filter can operate in either Sinc mode or FIR mode. Sinc mode has fourth-order Sinc1~Sinc4 options and its data rate range is 2.5~38400 SPS, while that of FIR mode is 2.5~20 SPS. Considering the noise performance and data rate of the system, the final filter is configured as Sinc4 mode with a data rate of 50 SPS. In this case, the noise of the ADC device is 96 nV and the noise-free bit is 21.7 bits.

E. Design of the power supply module

Fig. 9 shows the power supply module. The system is powered by 10000 mAh Li-on batteries and can operate continuously for 8 hours. The system is charged by the IP2312 charging module, which can reach a charging current of 3A and is fully charged in 2 hours. Depending on the different voltages required by the individual parts of the system, the battery voltage must be converted by the power chip and the 3.7 V of the Li-on batteries is regulated to 5 V by the TPS63020 low-ripple switching power supply to power the high-power display system and the Lora communication system. The voltage, temperature and power of the Li-on batteries are detected by the MAX10743 module and transmitted to the main control microcontroller STM32f407. The processed information is shown on the display screen or sent to the host computer for remote monitoring via Lora wireless communication. The PCB uses a digital-analog power isolation design, the digital circuit part is powered by the SPX3819-3.3 to supply power to the single-chip microcomputer and memory chip, while the analog circuit part SPX3819-5 and LT1175 and other chips supply a linear voltage of +5 V and -5 V to power the ADS1263 and conditioning circuit.

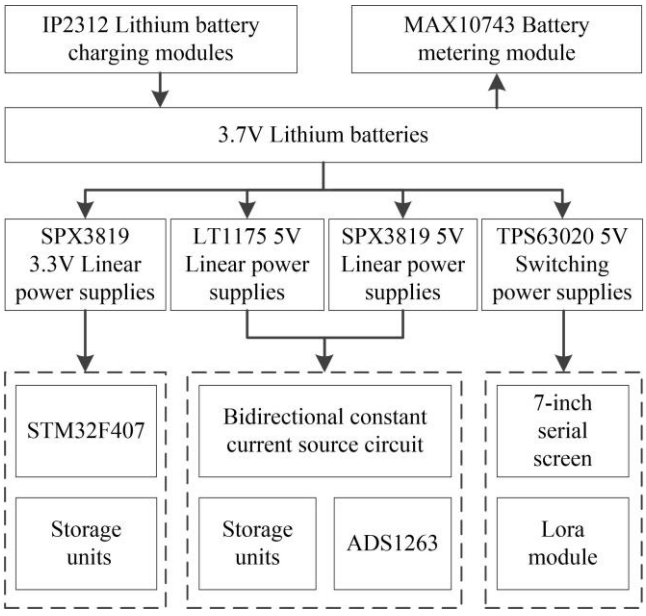

Fig. 9. Power supply module.

4. DESIGN OF SYSTEM SOFTWARE

A. Design of the main program

Fig. 10 shows the flow chart of the main calibration program for the temperature field in the thermostatic metal bath.

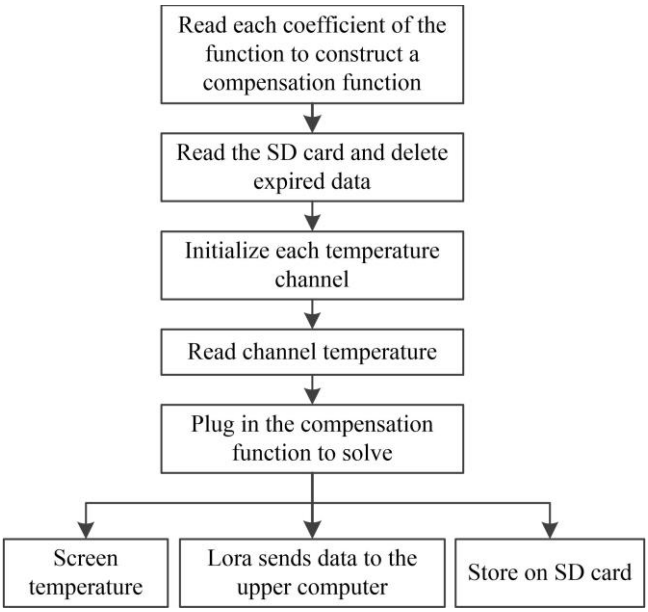

Fig. 10. Flow chart of the main program.

B. Processing of collected temperature data

To ensure the accuracy of the calibration set-up, it is necessary to perform a temperature calibration of the thermostatic metal bath temperature field calibration set-up. In the experiment, the temperature calibration of the pyrostat is performed by the intelligent super thermometer ConST685 and a standard Pt resistor to create a constant temperature environment. First, the metal bath calibration set-up requires the initial temperature setting. The Pt resistor of the device is inserted into a calibrated pyrostat and the initial AD (Analog to Digital) of the device is measured every 10 °C (i.e., 18 temperature measurement sites) at the calibration point -20 °C~150 °C. Then, AD is converted into temperature and stored on the chip. For the first temperature measurement, a part of the temperature point AD of each channel is measured. The AD values for the initial temperature measurements of each channel are listed in Table 3.

Since the AD of the temperature sensor corresponds to the temperature, the displayed value of the temperature and the temperature can be determined by the linear regression method to create a mathematical model according to the conversion formula. The least squares method is used to solve the problem. The initial fitting function is supposed to be a quadratic function when the temperature is greater than 0 °C, represented by (9), and a cubic function when the temperature is less than 0 °C, represented by (10):

$$t(x) = a_{10} + a_{11}x + a_{12}x^2 \tag{9}$$

$$t(x) = a_{20} + a_{21}x + a_{22}x^2 + a_{23}x^3 + a_{24}x^4 \tag{10}$$

where t is the temperature of the first fitting, x is the input AD, a_{10}, a_{11} and a_{12} are the primary conversion coefficients when it is greater than 0 °C, and a_{20}, a_{21}, a_{22}, a_{23} and a_{24} are the primary conversion coefficients when it is less than 0 °C.

The primary conversion coefficients are obtained by inserting AD into (9) and (10), and after fitting measurements are taken again every 10 °C at a temperature measurement site in the pyrostat -20 °C~150 °C. To eliminate the error, it is necessary to perform a segmental compensation of the temperature. The temperature range is divided into four segments: -20 °C~0 °C, 0 °C~50 °C, 50 °C~100 °C and 100 °C~150 °C for data compensation, respectively. This means that the three-stage temperature ranges are defined and the compensation formula is represented by (11):

$$\phi_i(t) = b_{i0} + b_{i1} + b_{i2}t^2 \tag{11}$$

where i represents the segment, φ_i is the temperature compensation value, t is the initial temperature, b_{i0}, b_{i1} and b_{i2} are the compensation coefficients.

Table 3. Initial temperature AD values.

Calibration temperature points	-20℃	0℃	50℃	100℃	150℃
Channel 1	999714649	1084849879	1296202819	1502711594	1708276185
Channel 2	999860908	1085002144	1296271205	1502788480	1708174566
Channel 3	999950816	1085129863	1296409593	1502942613	1708310643
Channel 4	999641440	1084800767	1296021625	1502562282	1707941734
Channel 5	999863219	1085050134	1296328523	1502877034	1708136384
Channel 6	1000000179	1085239761	1296510812	1503114624	1708430528
Channel 7	999774380	1085014869	1296129399	1502907797	1708081408
Channel 8	999898662	1085185004	1296477357	1503173354	1708500185
Channel 9	999863193	1085161933	1296488910	1503291840	1708355673
Channel 10	999542252	1084808177	1296037410	1502722773	1707611136
Channel 11	1000151564	1085381529	1294819294	1503559957	1708937369
Channel 12	999986950	1085261805	1296515247	1503208000	1708458380

Table 4. Temperature values from secondary fitting.

Temperature points	-20℃	0℃	50℃	100℃	150℃
Channel 1	-20.011	0.019	50.005	100.017	150.012
Channel 2	-20.021	0.011	50.007	100.005	150.001
Channel 3	-20.015	0.009	49.989	99.982	149.991
Channel 4	-20.010	0.006	50.001	100.010	150.009
Channel 5	-20.015	0.017	50.008	99.989	150.012
Channel 6	-20.012	0.012	50.011	100.005	150.013
Channel 7	-20.008	0.007	50.010	100.009	150.002
Channel 8	-20.011	0.019	50.006	100.010	150.006
Channel 9	-20.012	0.013	50.004	100.004	150.009
Channel 10	-19.996	-0.018	50.010	100.015	150.012
Channel 11	-20.008	0.010	50.006	100.019	150.011
Channel 12	-20.002	0.016	50.009	100.004	150.006

The coefficients b_{i0}, b_{i1} and b_{i2} are solved by quadratic fitting using the least squares method, and the final temperature conversion formula is a superposition of the compensation formula:

$$T = t + \phi \tag{12}$$

After correction, the pyrostat is measured again at -20 ℃, 0 ℃, 50 ℃, 100 ℃ and 150 ℃. The obtained temperatures are listed in Table 4.

5. CONCLUSIONS

In this paper, the requirements for the accuracy and reliability of temperature calibration in thermostatic metal baths and the status of the lack of dedicated temperature calibration devices when various types of metal bath modules appear in the calibration process are studied, and a thermostatic metal bath temperature field calibration system is designed. Using the finite element method to simulate the heating of the metal bath, it is found that the temperature distribution in the hole of the metal bath is relatively uniform, but the part close to the air is strongly affected. Therefore, a thermostatic block with good sealing performance was developed, which can be adapted to a metal bath module with different apertures, avoiding the influence of the environment on the measurement results, and different metal bath modules can be measured simultaneously to achieve accurate measurement of the metal bath temperature. In addition, a multi-channel temperature measurement system consisting of a sensor, a constant current source excitation unit, a signal conditioning unit, a high-precision temperature collection unit, a control and processing module and an interaction module has been developed. The system is corrected by piecewise linear fitting, and the error in the proposed temperature range is smaller than the standard requirement after experimental tests, which meets the calibration requirements of the thermostatic metal bath.

ACKNOWLEDGMENT

This work was supported by the Technology Innovation Center of Central Asia Energy Metrology for State Market Regulation (2021AEM01).

REFERENCES

[1] Zhang, Q., Zhou, S., Xu, H. (2018). Measurement uncertainty evaluation of temperature deviation of thermostatic metal bath. *Metrology & Measurement Technique*, 45 (12), 121-122. https://doi.org/10.15988/j.cnki.1004-6941.2018.12.040

[2] Luo, H., Gong, W. (2020). Research on calibration method for metal bath incubator. *Metrology & Measurement Technique*, 47 (12), 70-72. https://doi.org/10.15988/j.cnki.1004-6941.2020.12.023

[3] He, X., Zhu, T., Lv, J. (2021). Research on temperature calibration device of thermostatic metal bath. *Metrology & Measurement Technique*, 48 (11), 1-4. https://doi.org/10.15988/j.cnki.1004-6941.2021.11.001

[4] Tao, J., Julaiti, M., Luo, H., Guo, T., Wang, P., Ren, H. (2021). Design of high precision multichannel wearable body temperature measurement system based on negative temperature coefficient. *Science Technology and Engineering*, 21 (14), 5733-5741.

[5] Zhang, W., Yao, J., Tang, X., Chang, A. (2021). Design of high-precision temperature acquisition system with dual − ADC based on thermistor. *Instrument Technique and Sensor*, 9, 43-47.

[6] Hu, P., Shi, W., Mei, J. (2014). High precision Pt-resistance temperature measurement system. *Optics and Precision Engineering*, 22 (04), 988-995. https://doi.org/10.3788/OPE.20142204.0988

[7] Ding, J., Yang, S., Ye, S. (2018). A fast-multi-channel sub-millikelvin precision resistance thermometer readout based on the round-robin structure. *Measurement Science Review*, 18 (4), 138-146. https://doi.org/10.1515/msr-2017-0020

[8] Piechowski, L., Muc, A., Iwaszkiewicz, J. (2021). The precise temperature measurement system with compensation of measuring cable influence. *Energies*, 14 (24), 8214. https://doi.org/10.3390/en14248214

[9] Jovanović, J., Denić, D. (2021). Mixed-mode method used for Pt100 static transfer function linearization. *Measurement Science Review*, 21 (5), 142-149. https://doi.org/10.2478/msr-2021-0020

[10] Lv, M., Xia, B., Yang, Y., Lin, Z., Zhu, J. (2021). Research on temperature measurement system of thermal resistance based on least square parabola piecewise fitting. *Metrology & Measurement Technique,* 48 (8), 27-30. https://doi.org/10.15988/j.cnki.1004-6941.2021.8.010

[11] Jovanović, J., Denić, D. (2016). A cost-effective method for resolution increase of the twostage piecewise linear ADC used for sensor linearization. *Measurement Science Review*, 16 (1), 28-34. https://doi.org/10.1515/msr-2016-0005

[12] Radetić, R., Pavlov-Kagadejev, M., Milivojević, N. (2015). The analog linearization of Pt100 working characteristic. *Serbian Journal of Electrical Engineering*, 12 (3), 345-357. https://doi.org/10.2298/SJEE1503345R

[13] Chu, W., Liu, Z., Gu, Z., Jia, J. (2021). Simulation and analysis of the whole calibration system for multi-channel temperature measurement. *Computer Measurement & Control,* 29 (10), 32-37. https://doi.org/10.16526/j.cnki.11-4762/tp.2021.10.006

[14] Salminen, J., Sairanen, H., Grahn, P., Högström, R., Lakka, A., Heinonen, M. (2017). Characterization of the humidity calibration chamber by numerical simulations. *International Journal of Thermophysics*, 38 (84). https://doi.org/10.1007/s10765-017-2221-y

Received August 28, 2023
Accepted January 08, 2024